

# Effect of Substitution on the ESR Spectra and Electronic Ground State of ZnTPP Cation Radicals

Paresh C. Dave<sup>[a]</sup> and D. Srinivas<sup>\*[b]</sup>

**Keywords:** Zinc / Metalloporphyrins / Porphyrins / Cations / Radicals / ESR

Zinc(II) complexes of substituted tetraphenylporphyrins,  $\text{Zn}[\text{T}(\text{X}-\text{P})\text{P}]$ , where  $\text{X} = \text{H}$ ,  $p\text{-F}$ ,  $p\text{-Cl}$ ,  $m\text{-Cl}$ ,  $p\text{-CH}_3\text{O}$ , and  $m\text{-CH}_3\text{O}$ , have been synthesized and characterized. Peripheral substitution shows marked changes in the chemical shifts of the phenyl proton resonances and  $E_{1/2}$  values of the redox couples in the anodic region while the UV/Vis spectra are unaffected. The monocation radicals of these complexes are generated by chemical oxidation with bromine. The ESR spectra reveal the formation of two types of radical species,  $\text{Zn}[\text{T}(\text{X}-\text{P})\text{P}]^+\text{Br}^-$  (species **I**) and  $\text{Zn}[\text{T}(\text{X}-\text{P})(\text{Br}_n\text{-P})]^+\text{Br}^-$  (species **II**): Species **I** at 298 K shows a spectrum, with well-resolved bromine hyperfine features, characteristic of a  $^2\text{A}_{2u}$  electronic ground state while species **II**, except for the complex with  $\text{X} = m\text{-CH}_3\text{O}$ , shows a featureless, isotropic reson-

ance attributable to a  $^2\text{A}_{1u}$  state.  $\text{Zn}[\text{T}(m\text{-CH}_3\text{O-P})(\text{Br}_n\text{-P})]^+\text{Br}^-$ , on the other hand, exhibits nine resolved nitrogen hyperfine features corresponding to a  $^2\text{A}_{2u}$  state. Variable temperature ESR spectra (77–298 K) indicate reduction in the bromine and nitrogen hyperfine coupling constants and an increase in the  $g$  value of species **I** from 2.0049 to 2.0060 with lowering temperature and suggest a labile electronic ground state for species **I**. The  $p\text{-CH}_3\text{O}$  substituted complex exhibits an electronic transformation from  $^2\text{A}_{2u}$  to  $^2\text{A}_{1u}$  while the remaining complexes, including  $m\text{-CH}_3\text{O}$ , show a transformation from  $^2\text{A}_{2u}$  to an admixed  $^2\text{A}_{1u}/^2\text{A}_{2u}$  state. The effect of substitution on the variable temperature ESR spectra are discussed.

## Introduction

Porphyrin  $\pi$ -cation radicals play a crucial role in the mechanisms of various biocatalytic reactions, including oxygen activation by heme proteins,<sup>[1–9]</sup> and in the electron-transfer processes at the photosynthetic reaction centre.<sup>[10,11]</sup> Based on the electronic ground state, the  $\pi$ -cation radicals have been categorised into those possessing a  $^2\text{A}_{1u}$  or a  $^2\text{A}_{2u}$  ground state.<sup>[9]</sup> The two highest occupied molecular orbitals of metalloporphyrins ( $a_{1u}$  and  $a_{2u}$ ) are nearly degenerate and their relative energies are dictated by many factors, including the nature and position of the porphyrin peripheral substitution, the central metal ion, the identity and disposition of the axial ligand, environment, temperature and symmetry of the molecule.<sup>[12–18]</sup> Compound **I** of catalase and chloroperoxidase enzymes belong to the former category of radicals.<sup>[7]</sup> The electronic ground state of compound **I** of horseradish peroxidase enzyme is still to be conclusively determined. ENDOR and magnetic circular dichroism studies have indicated a  $^2\text{A}_{2u}$  ground state for HRP-I<sup>[19,20]</sup> while more recent NMR<sup>[21,22]</sup> and Resonance Raman (RR)<sup>[23,24]</sup> studies show a  $^2\text{A}_{1u}$  state. A correlation between the electronic structure and functionality is interesting, but so far not conclusive and therefore needs further work.<sup>[2]</sup>

Generally, among the synthetic metalloporphyrins, the cation radicals of the octaethylporphyrins  $\text{M}\{\text{OEP}\}^{+\cdot}$  pos-

sess a  $^2\text{A}_{1u}$  ground state while those of the tetraphenylporphyrins  $\text{M}\{\text{TPP}\}^{+\cdot}$  possess a  $^2\text{A}_{2u}$  state ( $\text{M} = \text{Zn}^{2+}$  and  $\text{Mg}^{2+}$ ).<sup>[1,9,25,26]</sup> However, it was found that  $\text{Co}\{\text{OEP}\}^{+\cdot}$  and  $\text{Ru}\{\text{OEP}\}^{+\cdot}$  have a  $^2\text{A}_{1u}$  ground state with  $\text{Br}^-$  as the counter ion and  $^2\text{A}_{2u}$  with  $\text{ClO}_4^-$  as the counter ion.<sup>[21,27]</sup> The electron density is greater at the *meso* carbon atoms in the case of the  $^2\text{A}_{2u}$  configuration, and hence electron-withdrawing substituents on the tetraphenyl groups of  $\text{M}\{\text{TPP}\}^{+\cdot}$  affect the energetics of  $a_{2u}$  while  $a_{1u}$  is unaltered. On the other hand, for radicals with a  $^2\text{A}_{1u}$  electronic ground state, the electron density is greater at the  $\beta$  carbon atoms of the pyrrole ring while the *meso* carbons lie in the nodal plane, and hence substitution on the pyrrole ring alters the position of the  $a_{1u}$  level while  $a_{2u}$  is hardly affected. Therefore, by a rational substitution it is possible, in principle, to design a molecule with a desired property.

Gross and co-workers have reported an admixed ground state for zinc complexes of halogen-substituted tetraphenylporphyrin cation radicals.<sup>[28,29]</sup> The quantum admixture of  $^2\text{A}_{1u}$  and  $^2\text{A}_{2u}$  states was also reported by Kalsbeck et al.<sup>[30]</sup> for  $\text{Zn}[\text{T}(\text{Cl}_2\text{-P})\text{P}]^{+\cdot}$  and  $\text{Mg}\{\text{T}(\text{Cl}_2\text{-P})\text{P}\}^{+\cdot}$  radicals where  $\text{T}(\text{Cl}_2\text{-P})\text{P}$  = tetrakis(*o*-dichlorophenyl)porphyrin. Theoretical studies on the  $\pi$ -cation radicals of metalloporphyrins have shown that electron-withdrawing substituents in the *meso* position lead to a  $^2\text{A}_{1u}$  ground state while electron-donating substituents result in a  $^2\text{A}_{2u}$  state.<sup>[31]</sup> Density functional calculations have revealed that electron-withdrawing substituents in the *meta* and *para* positions should exert significantly stronger electronic effects than with *ortho* substitution.<sup>[32]</sup> Our recent studies using variable temperature ESR spectroscopy indicated, for the first time, a labile electronic ground state for  $\text{Zn}[\text{T}(\text{H-P})\text{P}]^+\text{Br}^-$  with a  $^2\text{A}_{2u}$

<sup>[a]</sup> Sophisticated Analytical Instruments Laboratory, Central Salt Marine Chemicals Research Institute, Gijubhai Badheka Marg, Bhavnagar 364 002, India

<sup>[b]</sup> Catalysis Division, National Chemical Laboratory, Pune 411 008, India  
Fax: (internat.) +91-20/589-3761  
E-mail: srinivas@cata.ncl.res.in

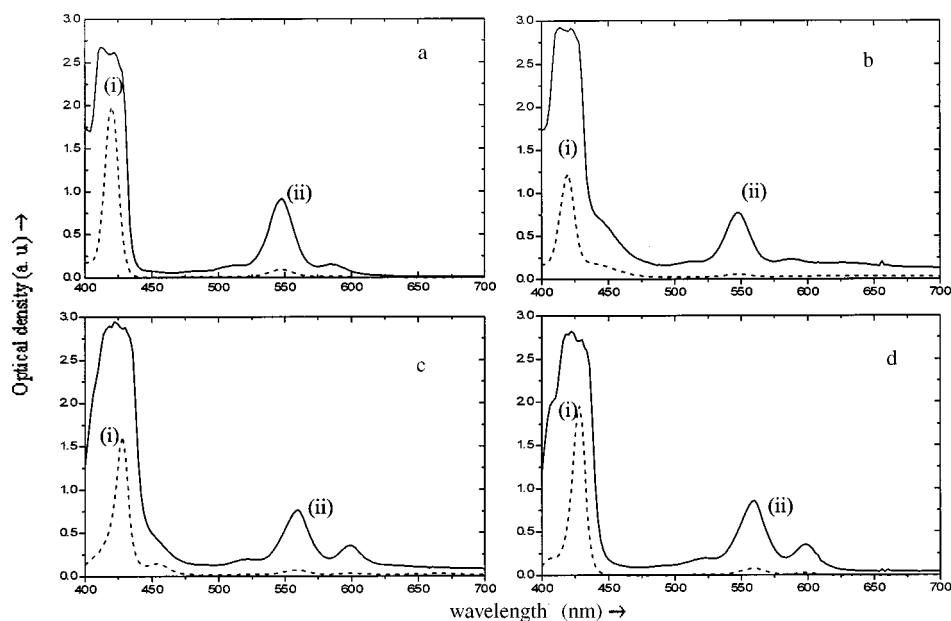


Figure 1. UV/Visible spectra for  $\text{Zn}[\text{T}(m\text{-CH}_3\text{O-P})\text{P}]$  in  $\text{CH}_2\text{Cl}_2$ : (a) neutral species, (b) cation radical, (c) cation radical + pyrazine, and (d) neutral species + pyrazine; (i) spectrum for 10 times lower concentration and (ii) for higher concentrations; optical density is in units of  $\text{mol}\cdot\text{cm}^{-1}$

ground state at 298 K changing to a  ${}^2\text{A}_{1\text{u}}$  state at 77 K.<sup>[33]</sup> In the course of understanding the factors influencing the electronic structure and structure-reactivity correlations, we here report the effect of peripheral substitution (X) on the ESR spectral properties and ground state configuration of  $\text{Zn}[\text{T}(\text{X-P})\text{P}]^+\text{Br}^-$  radical cations generated by chemical oxidation with bromine. Two types of radical species viz.,  $\text{Zn}[\text{T}(\text{X-P})\text{P}]^+\text{Br}^-$  (I) and  $\text{Zn}[\text{T}(\text{X-P})(\text{Br}_n\text{-P})]^+$ ,  $n = 8$  or 4 (II and II', respectively) are observed on oxidation with bromine. Irrespective of the nature of the peripheral substitution ( $\text{X} = p\text{-CH}_3\text{O}$ ,  $p\text{-Cl}$ ,  $p\text{-F}$ ,  $m\text{-CH}_3\text{O}$ ,  $m\text{-Cl}$ ), species I showed a labile electronic ground state ( ${}^2\text{A}_{2\text{u}}$  at 298 K and  ${}^2\text{A}_{1\text{u}}$  or admixed  ${}^2\text{A}_{1\text{u}}/{}^2\text{A}_{2\text{u}}$  at 77 K). Species II, however, is  ${}^2\text{A}_{1\text{u}}$  throughout the temperature range 77–298 K, although species II' exhibits ground state lability similar to that of species I. The changes in the electronic structure are proposed to be associated with the changes in the conformational geometry of the porphyrin skeleton. It is to be noted that the notations  ${}^2\text{A}_{1\text{u}}$  and  ${}^2\text{A}_{2\text{u}}$  assume  $D_{4\text{h}}$  symmetry for the porphyrin cores. These notations are used here only for simplicity as the porphyrin cores of the molecules studied in this work have a symmetry lower than  $D_{4\text{h}}$ .

## Results and Discussion

A typical UV/Vis spectrum for  $\text{Zn}[\text{T}(m\text{-CH}_3\text{O-P})\text{P}]$  is shown in Figure 1 a. Substituents have little effect and showed similar UV/Vis spectra for all the complexes. In strong donor solvents and in the presence of nitrogenous ligands, such as pyridine, imidazole and pyrazine (Figure 1 d), the Soret and Q-bands are red shifted indicating a change in molecular conformation, probably due to solvation and axial ligand coordination. The cation radicals of  $\text{Zn}[\text{T}(\text{X-P})\text{P}]$ , generated by chemical oxidation with brom-

ine, showed a blue-shift and reduced intensity for the Soret band and broad, diffused, overlapping Q-bands in the region 500–700 nm (Figure 1 b). These spectral features are characteristic of a  ${}^2\text{A}_{2\text{u}}$  ground state of the porphyrin cation radical.<sup>[25,26]</sup> Upon adding nitrogenous ligands to the radical solution, a spectrum typical of the neutral species was observed, indicating the instability of cation radicals in the presence of coordinating ligands (Figure 1 c). This agrees well with the RR results on some iron tetraphenylporphyrin cation radicals.<sup>[34]</sup>

The effect of substitution is clearly manifested on the chemical shifts of the phenyl proton resonances; the signals due to the  $\beta$ -protons are unaffected. These resonances were shifted up-field due to the substitution. This shift, with *para* substitution, was marginal for the *ortho* protons and varies in the sequence  $\text{H} < \text{F} < \text{Cl} < \text{OCH}_3$  while it was significant for the *meta* protons where it varies in the order  $\text{H} < \text{Cl} < \text{F} < \text{OCH}_3$ . Similar trends were also observed with *meta* substitution. The  ${}^1\text{H}$ -NMR spectroscopic data for all the complexes are listed in Table 1. The trends described for the chemical shifts are completely in line with what is expected for phenyl protons and simply show that there is practically no conjugation between the porphyrin and the phenyl groups, as they are probably perpendicular to one other.

Cyclic voltammograms (CVs) of the complexes showed two quasi-reversible redox couples in the range 0 to +2.0 V, corresponding to  $\text{Zn}[\text{T}(\text{X-P})\text{P}]^+/\text{Zn}[\text{T}(\text{X-P})\text{P}]$  and  $\text{Zn}[\text{T}(\text{X-P})\text{P}]^{2+}/\text{Zn}[\text{T}(\text{X-P})\text{P}]^+$ , respectively. Representative CV and differential pulse voltammograms (DPV) for  $\text{Zn}[\text{T}(m\text{-CH}_3\text{O-P})\text{P}]$  are shown in Figure 2 and the electrochemical data are provided in Table 2. Ferrocene was used as the reference. The  $E_{1/2}$  values vary with the substituents in the order  $\text{F} > \text{Cl} > \text{H} > \text{OCH}_3$ . Electron donating

Table 1.  $^1\text{H}$  NMR spectroscopic data for Zinc(II) complexes of substituted tetraphenylporphyrins  $\text{Zn}[\text{T}(\text{X}-\text{P})\text{P}]$  in  $\text{CDCl}_3$ 

X	Pyrrole	<i>o</i> -	<i>m</i> -	<i>p</i> -
H	8.95	8.27, 8.25, 8.18	7.78, 7.76, 7.72	—
<i>p</i> -OCH <sub>3</sub>	8.85	8.15, 8.11	7.30, 7.2	4.07(OCH <sub>3</sub> )
<i>m</i> -OCH <sub>3</sub>	8.97	7.79, 7.77	7.33, 7.32, 7.29, 7.28	7.66, 7.62, 7.59, 3.95(OCH <sub>3</sub> )
<i>p</i> -Cl	8.93	8.16, 8.12	7.78, 7.76, 7.72	—
<i>p</i> -F	8.93	8.20, 8.17, 8.16, 8.13	7.50, 7.45, 7.41	—
<i>m</i> -Cl	8.95	8.22, 7.82, 7.78	7.73, 7.69, 7.65	8.12, 8.09

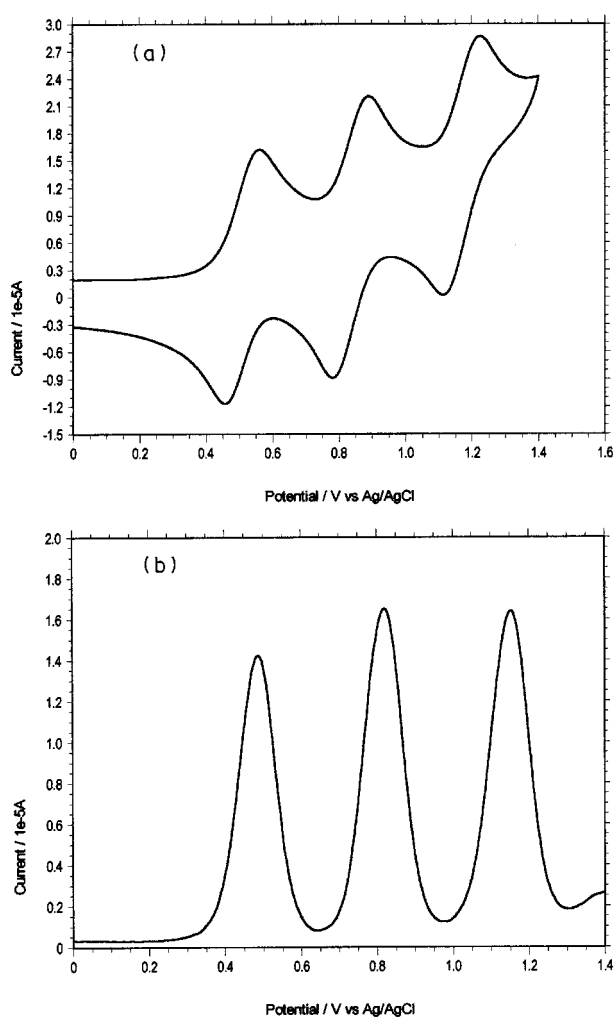


Figure 2. (a) CV (b) DPV of  $\text{Zn}[\text{T}(\text{m}-\text{CH}_3\text{O}-\text{P})\text{P}]$  in  $\text{CH}_2\text{Cl}_2$ ; working electrode: glassy carbon; reference electrode:  $\text{Ag}/\text{AgCl}$ ; auxiliary electrode: Pt wire; supporting electrolyte: tetrabutylammonium hexafluorophosphate; scan rate: 100 mV/s; the first couple at  $E_{1/2} = 0.51$  V corresponds to the redox couple of ferrocene used as an internal reference

Table 2. Electrochemical data for 0.1 M  $\text{Zn}[\text{T}(\text{X}-\text{P})\text{P}]$  in  $\text{CH}_2\text{Cl}_2$ 

Complex	$E_{1/2}^1$	$E_{1/2}^2$
$\text{Zn}[\text{T}(\text{p}-\text{F}-\text{P})\text{P}]$	0.95	1.42
$\text{Zn}[\text{T}(\text{m}-\text{Cl}-\text{P})\text{P}]$	0.95	1.26
$\text{Zn}[\text{T}(\text{p}-\text{Cl}-\text{P})\text{P}]$	0.93	1.2
$\text{Zn}[\text{T}(\text{H}-\text{P})\text{P}]$	0.89	1.35
$\text{Zn}[\text{T}(\text{m}-\text{OCH}_3-\text{P})\text{P}]$	0.84	1.17
$\text{Zn}[\text{T}(\text{p}-\text{OCH}_3-\text{P})\text{P}]$	0.82	1.23

$\text{CH}_3\text{O}$  substitution means that the oxidation is easier than with the electron-withdrawing halogen groups. The  $E_{1/2}$  of the *meta*-substituted porphyrins is larger than that of the *para*-substituted porphyrins. The  $E_{1/2}$  for couple **II**,  $\text{Zn}[\text{T}(\text{X}-\text{P})\text{P}]^{2+}/\text{Zn}[\text{T}(\text{X}-\text{P})\text{P}]^{+}$  is more affected by the substitution than couple **I**,  $\text{Zn}[\text{T}(\text{X}-\text{P})\text{P}]^{+}/\text{Zn}[\text{T}(\text{X}-\text{P})\text{P}]$ . The trends in  $E_{1/2}$  are as expected, as are the chemical shifts.

The ESR spectra of the cation radicals, in general, consist of four equally spaced resolved hyperfine (h.f.) features. The intensity of the third h.f. feature is greater than expected. Spectral simulations indicate the presence of two types of paramagnetic radical species; species **I** showing the characteristic four line h.f. pattern due to interaction of electron spin ( $S = 1/2$ ) with the nuclear spin ( $I$ ) of  $3/2$  and species **II** exhibiting an isotropic resonance. For species **I**, the coupling is due to coordinated bromide ion.<sup>[35]</sup> The intensity of the signal due to species **II** increased with excess bromine. Species **I** could be attributed to  $\text{Zn}[\text{T}(\text{X}-\text{P})\text{P}]^{+}\text{Br}^{-}$  and **II** to brominated cation radicals,  $\text{Zn}[\text{T}(\text{X}-\text{P})(\text{Br}_n-\text{P})]^{+}\text{Br}^{-}$ . Depending on the type of substitution (X) and its location (*para/meta*) the value of “*n*” can be 8 or 4.<sup>[36]</sup> Figure 3 shows a schematic representation of various oxidation products and their nomenclature. Two types of tetrabromotetraphenylporphyrin cation radicals (species **II'**) are possible, as shown in Figure 3, one with one bromine substituent per pyrrole ring and the others with two bromine substituents on the two opposing pyrrole rings.  $^1\text{H}$ -NMR spectroscopic studies by Crossley et al. favour the formation of the latter species with two bromine substituents on the two opposing pyrrole rings in the reaction of metal-free tetraphenylporphyrin with *N*-bromosuccinimide.<sup>[37]</sup>

The UV/Visible spectrum and the resolved h.f. coupling features of species **I** at ambient temperatures are characteristic of a  $^2\text{A}_{2u}$  electronic ground state while the featureless isotropic signal for species **II** is characteristic of a  $^2\text{A}_{1u}$  state. Upon sudden lowering of the temperature to 77 K, the h.f. features disappeared and, instead, only two overlapping isotropic resonances for species **I** and **II** or **II'** were visible. Representative spectra for the cation radicals of  $\text{Zn}[\text{T}(\text{p}-\text{CH}_3\text{O}-\text{P})\text{P}]$  and  $\text{Zn}[\text{T}(\text{m}-\text{CH}_3\text{O}-\text{P})\text{P}]$  at 298 and 77 K along with the simulated results are shown in Figure 4 and Figure 5, respectively.

The spin Hamiltonian parameters for all the radicals are listed in Table 3. Except for  $\text{Zn}[\text{T}(\text{m}-\text{CH}_3\text{O}-\text{P})\text{P}]$ , the peak-to-peak linewidth ( $\Delta H$ ) increased from 5.5 to 8.0 G for species **II** while it decreased from 8.9 to 8.0 G for species **I** with lowering of the temperature. The *g* value increased from 2.0048 to 2.0057 and  $A_{\text{Br}}$  increased from 7.61 to 8.30

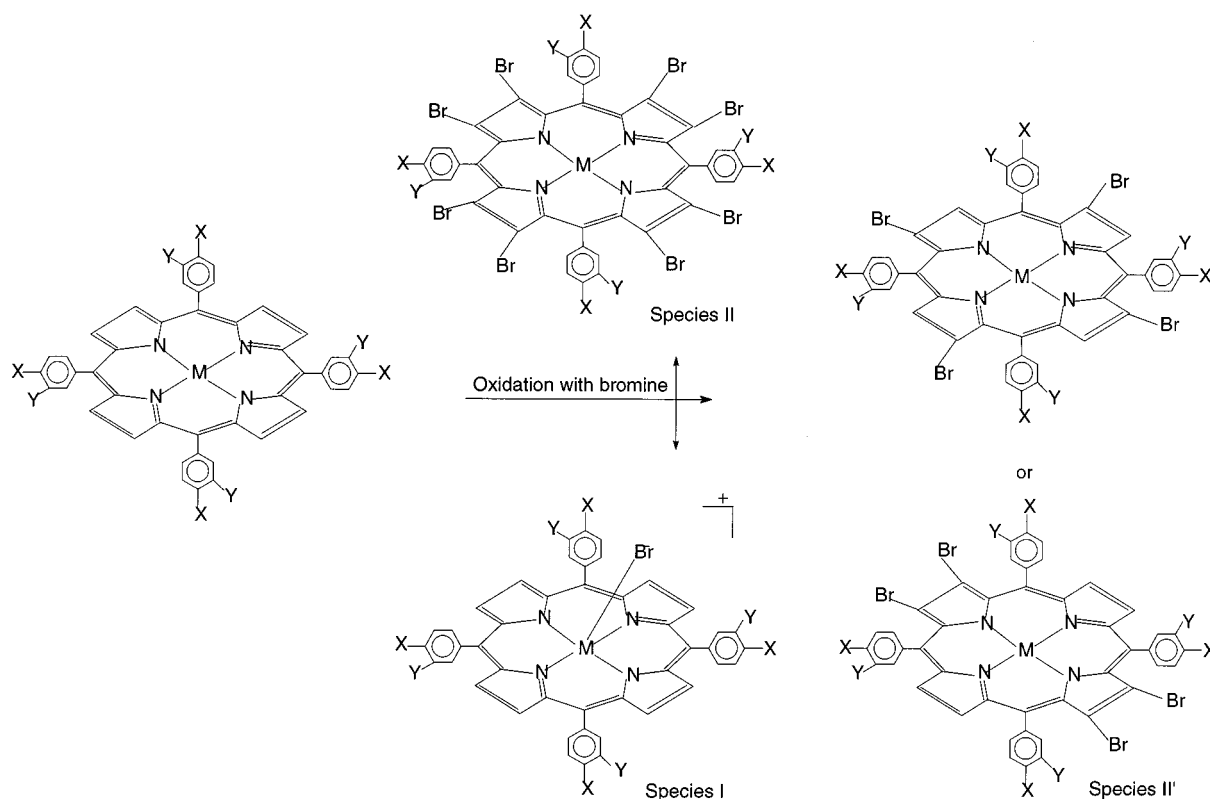


Figure 3. Schematic representation of various oxidation products of  $\text{Zn}[\text{T}(\text{X-P})\text{P}]$

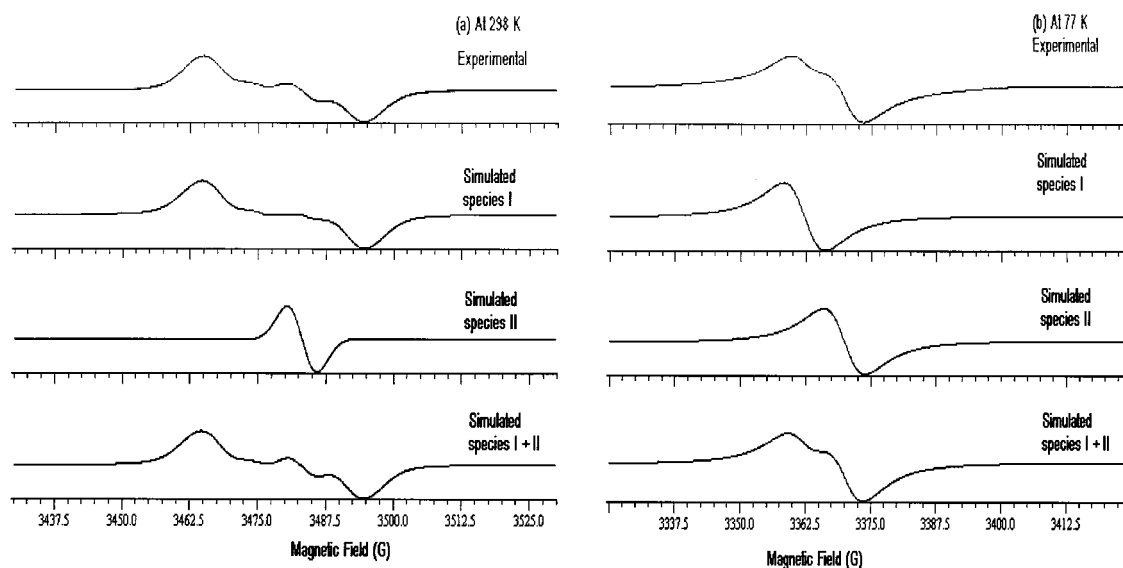


Figure 4. Experimental and simulated ESR spectra of  $\text{Zn}[\text{T}(\text{p-CH}_3\text{O-P})\text{P}]$  in  $\text{CH}_2\text{Cl}_2$  at 298 and 77 K; receiver gain =  $5.02 \cdot 10^3$ , modulation amplitude = 0.6 G, power = 2 mW, time constant = 81.92 ms,  $\nu = 9.76$  GHz (for 298 K) 9.46 GHz (for 77 K) and resolution in  $X = 1024$

G with the increasing electron-withdrawing capacity of the substituent. The location of the substituent (*para* or *meta*) has a considerable effect on the  $A_{\text{Br}}$  value. This value increased from 7.61 to 8.20 for  $\text{CH}_3\text{O}$  substitution and decreased from 8.30 to 8.10 G for chloro substitution. The disappearance of the bromine h.f. coupling features at 77 K is attributed to a change in the electronic ground state from  $^2A_{2u}$  to  $^2A_{1u}$  for species I. A systematic variation of temper-

ature in the range 298 K to 77 K, discussed below, for the cation radicals of  $\text{Zn}[\text{T}(\text{p-CH}_3\text{O-P})\text{P}]$  and  $\text{Zn}[\text{T}(\text{m-CH}_3\text{O-P})\text{P}]$ , provides a deeper insight into the transition behavior.

Figure 6 shows the variable temperature ESR spectra for the cation radicals of  $\text{Zn}[\text{T}(\text{p-CH}_3\text{O-P})\text{P}]$  and  $\text{Zn}[\text{T}(\text{m-CH}_3\text{O-P})\text{P}]$ . Bromine h.f. coupling constant ( $A_{\text{Br}}$ ) for species I decreased gradually as the temperature was lowered

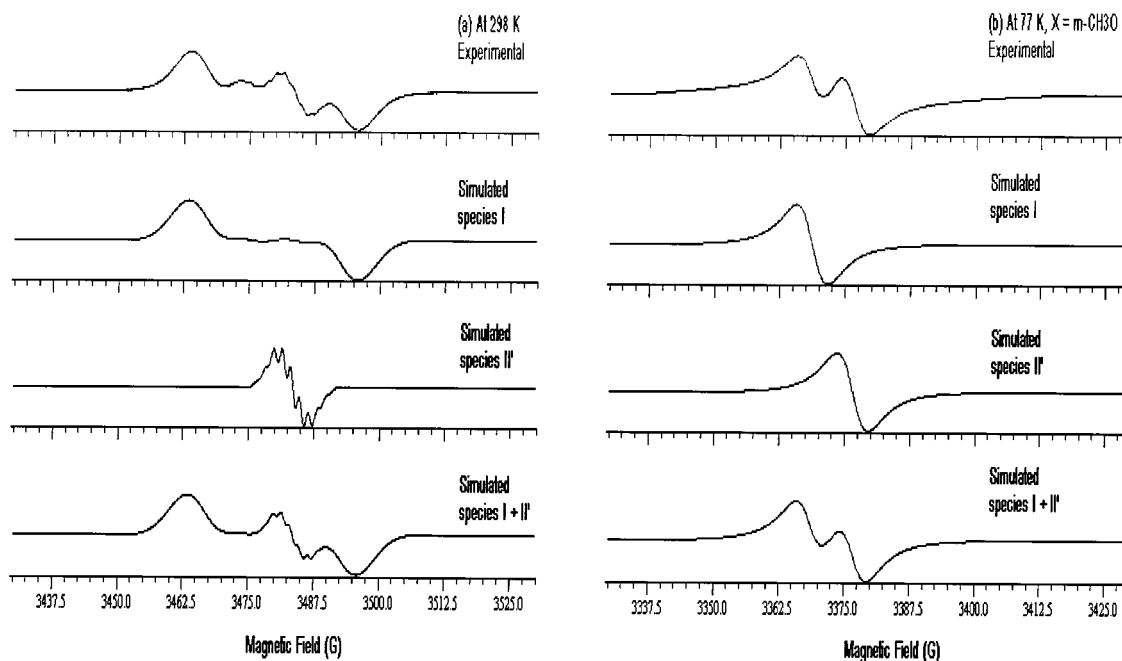


Figure 5. Experimental and simulated ESR spectra of Zn[T(*m*-CH<sub>3</sub>O-P)P] in CH<sub>2</sub>Cl<sub>2</sub> at 298 and 77 K; receiver gain =  $5.02 \cdot 10^3$ , modulation amplitude = 0.6 G, power = 2 mW, time constant = 81.92 ms,  $\nu$  = 9.76 GHz (for 298 K) 9.46 GHz (for 77 K) and resolution in X = 1024

Table 3. Simulated EPR data for monocation radicals of Zinc(II) substituted tetraphenylporphyrins, Zn[T(X-P)P]<sup>+</sup>, in CHCl<sub>3</sub>

X	Temp. [K]	[g]	Species I A(Br) [G]	$\Delta H$ [G]	[g]	Species II $\Delta H$ [G]
<i>p</i> -CH <sub>3</sub> O	298	2.0048	7.61	8.5	2.0028	5.5
	77	2.0075	—	8.0	2.0029	8.0
H	298	2.0050	8.15	8.8	2.0028	5.5
	77	2.0078	—	8.0	2.0019	8.0
<i>p</i> -F	298	2.0052	8.20	8.8	2.0030	5.5
	77	2.0080	—	8.0	2.0033	8.0
<i>p</i> -Cl	298	2.0055	8.30	8.9	2.0032	5.5
	77	2.0074	—	8.2	2.0037	8.1
<i>m</i> -CH <sub>3</sub> O	298	2.0052	8.20	8.6	2.0030	1.50
	77	2.0080	—	6.0	2.0033	6.0
<i>m</i> -Cl	298	2.0057	8.10	8.25	2.0035	5.5
	77	2.0076	—	8.4	2.0039	7.4

from 298 to 190 K, in steps of 10 K and from then onwards showed a featureless isotropic resonance.

However, distinct changes were observed for species II with the *p*-CH<sub>3</sub>O and *m*-CH<sub>3</sub>O substituted complexes. The former, like the rest of the complexes, showed a featureless isotropic resonance throughout the temperature range, the latter complex with *m*-CH<sub>3</sub>O substitution, on the other hand, showed nine well-resolved hyperfine features ( $\Delta H$  = 1.70 G) due to interaction of the electron spin with the nuclear spin of four equivalent nitrogen atoms ( $I$  = 1). The spectral behaviour and the  $A_N$  value (1.56 G) are consistent with those of TPP radicals with ClO<sub>4</sub><sup>−</sup> as the counterion.<sup>[26]</sup> Theoretical calculations for the <sup>2</sup>A<sub>2u</sub> ground state revealed a larger electron density at the pyrrole nitrogen and meso carbon atoms and negligible electron density at the  $\beta$  pyrrole position. For the <sup>2</sup>A<sub>1u</sub> ground state the pyrrole nitrogens and the meso carbons are in the nodal plane and the

electron density is greater at the  $\beta$ -pyrrole position. Hence, a resolved, hyperfine-rich spectrum is observed for the cation radical with a <sup>2</sup>A<sub>2u</sub> ground state while a featureless isotropic signal is observed for the <sup>2</sup>A<sub>1u</sub> ground state. Variable temperature ESR results in the present study therefore indicate a <sup>2</sup>A<sub>2u</sub> electronic ground state for species II' with *m*-CH<sub>3</sub>O substitution and <sup>2</sup>A<sub>1u</sub> for the rest of the complexes. As the temperature is lowered the h.f. resolution is lost. Figure 7 shows the variation of  $A_{Br}$  and  $\Delta H/A_{Br}$  with temperature for Zn[T(*m*-CH<sub>3</sub>O-P)P] cation radicals.

The former radical shows an abrupt change around 180 K while for the latter the bromine hyperfine coupling is reduced gradually up to 77 K. The rate of cooling has an effect on the nature of the spectrum. Sudden cooling to 77 K gives an overlapping two line spectrum for *p*-CH<sub>3</sub>O substitution (Figure 5) whereas slow cooling shows a single resonance. However, such a behaviour is not observed for the complexes with X = *m*-CH<sub>3</sub>O and H. These observations clearly indicate that the cation radical of Zn[T(*p*-CH<sub>3</sub>O-P)P] (species I) undergoes an electronic transition from <sup>2</sup>A<sub>2u</sub> to <sup>2</sup>A<sub>1u</sub> at 180 K while the rest of the complexes exhibit a transition from <sup>2</sup>A<sub>2u</sub> to an admixed <sup>2</sup>A<sub>1u</sub>/<sup>2</sup>A<sub>2u</sub> state as the temperature is lowered. The reduction in the bromine hyperfine coupling constant at lower temperatures indicates a change in the degree of binding of the bromine ion in the Zn[T(X-P)P]<sup>+</sup>Br<sup>−</sup> complex. Our earlier studies<sup>[33]</sup> revealed that the Zn–Br bond is labile and the Br<sup>−</sup> could be replaced by ClO<sub>4</sub><sup>−</sup>, PF<sub>6</sub><sup>−</sup>, and BF<sub>4</sub><sup>−</sup> ions. The perchlorato anion forms an axial coordination and shows a typical spectrum with a nine line hyperfine pattern due to interaction with the four equivalent nitrogen atoms of the pyrrole rings. With noncoordinating PF<sub>6</sub><sup>−</sup> and BF<sub>4</sub><sup>−</sup> ions, however, only a single line is observed.



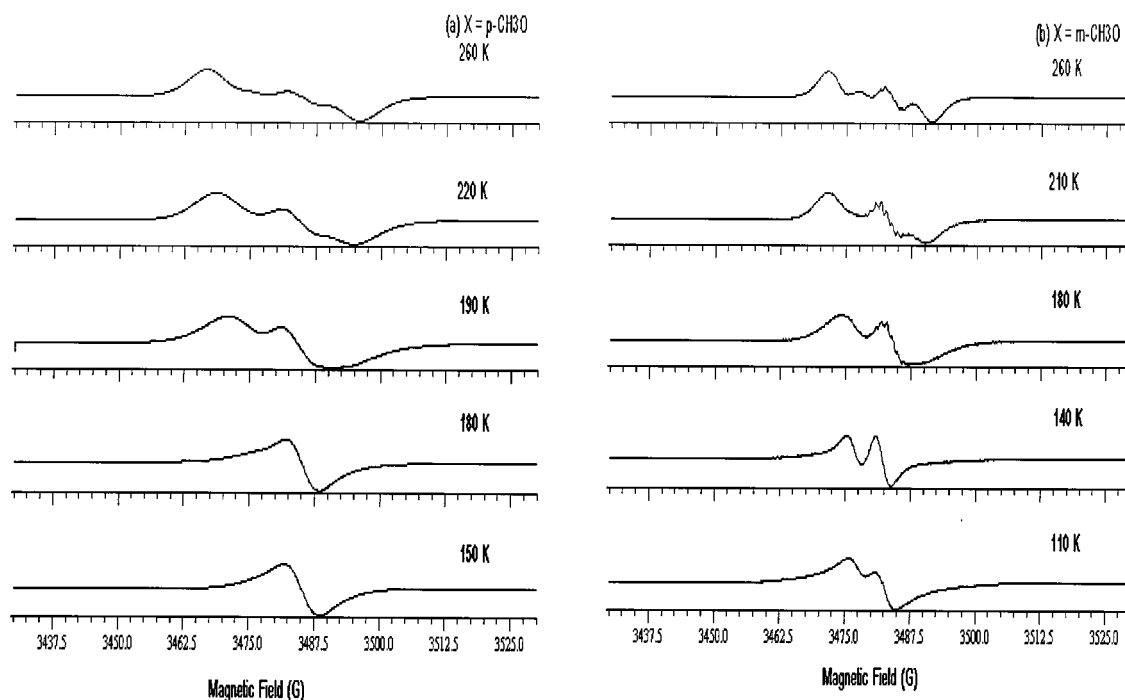


Figure 6. Variable temperature ESR spectra for (a)  $\text{Zn}[\text{T}(p\text{-CH}_3\text{O-P})\text{P}]$  and (b)  $\text{Zn}[\text{T}(m\text{-CH}_3\text{O-P})\text{P}]$  in  $\text{CH}_2\text{Cl}_2$  showing the effect of substitution on the lability of the electronic ground state; species **II** shows resolved nitrogen hyperfine coupling for *m*- $\text{CH}_3\text{O}$  (b) while a featureless signal is seen for *p*- $\text{CH}_3\text{O}$  (a) substituted complexes; receiver gain =  $5.02 \cdot 10^3$ , modulation amplitude = 1.60 G, time constant = 163.84 ms,  $\nu = 9.46$  GHz, resolution in X = 1024

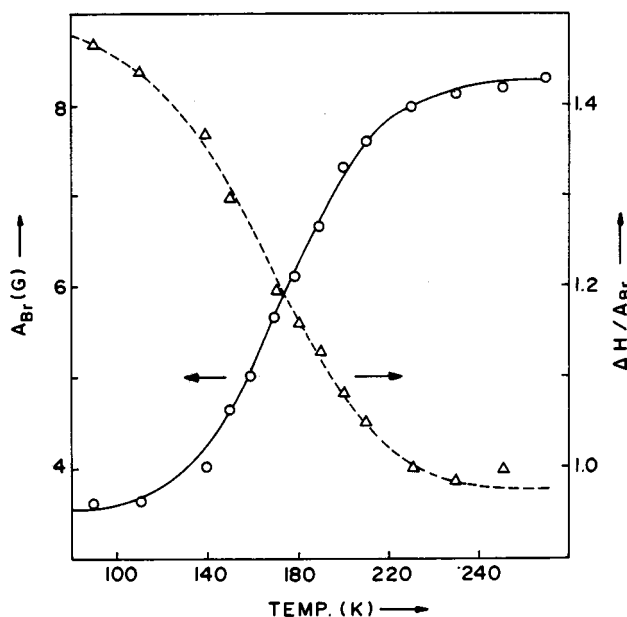


Figure 7. Variation of  $A_{\text{Br}}$ ,  $\Delta H/A_{\text{Br}}$  with temperature for  $\text{Zn}[\text{T}(m\text{-CH}_3\text{O-P})\text{P}]^+\text{Br}^-$

Species **II**, as mentioned earlier, is attributed to a brominated species,  $\text{Zn}[\text{T}(\text{X-P})(\text{Br}_n\text{-P})]^+\text{Br}^-$ .<sup>[36]</sup> The difference in the spectral features of the *m*- $\text{CH}_3\text{O}$  substituted complex (showing resolved nitrogen hyperfine coupling) from the rest of the complexes is attributed solely to the location of the substituent and its electronic and steric effects. During chemical oxidation both the  $\beta$ -pyrrole positions can be brominated resulting in species **II**. However, bulkier  $\text{CH}_3\text{O}$  sub-

stitution in the *meta* position probably imposes a degree of steric hindrance and thereby forms a tetrabrominated cation radical (species **II'**) instead of the octabrominated species **II**. The former, with an electron-donating  $\text{CH}_3\text{O}$  group in the *meta* position and electron-withdrawing tetrabromo groups in the  $\beta$ -pyrrole position, stabilizes the  $^2A_{2u}$  ground state while the rest of the substituted complexes with octabromo substitution in the  $\beta$ -pyrrole position stabilize the  $^2A_{1u}$  state for species **II**. As for all the structures of the octabrominated tetraphenylporphyrin complexes studied so far, species **II** most probably possesses an  $S_4$  symmetry and displays a saddle-shaped or ruffled conformation.<sup>[38]</sup> Such a nonplanar conformation probably stabilizes a  $^2A_{1u}$  electronic ground state. As reported earlier,<sup>[38]</sup> the symmetry of the tetrabrominated cation radical (species **II'**) is expected to be, at least,  $C_i$  with slightly distorted chair-like conformation and such a geometry probably stabilizes a  $^2A_{2u}$  state. With lowering of temperature, the conformational geometries of species **I** and **II'** change and this results in a transition in the electronic ground state from  $^2A_{2u}$  to  $^2A_{1u}$ . Hence, it can be concluded that the lability in the electronic structure is associated with a change in the conformational geometry of the TPP moiety.

## Conclusions

Chemical oxidation of zinc(II) substituted tetraphenylporphyrins with bromine generated two types of cation radicals,  $\text{Zn}[\text{T}(\text{X-P})\text{P}]^+\text{Br}^-$  (species **I**) and  $\text{Zn}[\text{T}(\text{X-P})(\text{Br}_n\text{-P})]^+\text{Br}^-$  (species **II**).

P)]<sup>+</sup>Br<sup>−</sup> (species **II** or **II'**). Species **I** for all the complexes exhibits a labile electronic ground state with a *p*-CH<sub>3</sub>O substituted radical ion showing an electronic transition from <sup>2</sup>A<sub>2u</sub> to <sup>2</sup>A<sub>1u</sub> while the rest of the radical ions show a transition from <sup>2</sup>A<sub>2u</sub> to an admixed <sup>2</sup>A<sub>1u</sub>/<sup>2</sup>A<sub>2u</sub> state. Species **II** with octabromo substitution at β-pyrrole position possesses a <sup>2</sup>A<sub>1u</sub> state throughout the temperature range (298–77 K), while the *m*-CH<sub>3</sub>O complex with tetrabromo substitution (species **II'**) exhibits a labile <sup>2</sup>A<sub>2u</sub> electronic state. The lability in the electronic state is associated with changes in the conformational geometry of the porphyrin macrocyclic moiety. Metal complexes with labile electronic ground states and flexible ligand geometries are potential materials for molecular devices. By and large the present study reveals that by incorporating an appropriate substitution into the porphyrin macrocycle it is possible to fine-tune the electronic structure to design a desired material.

## Experimental Section

**Materials:** Aldehydes and other chemicals (E. Merck) were used as received. Solvents (A.R. grade) were purified and dried before use. Freshly distilled pyrrole (Aldrich) was used for the condensation.

**Physical Measurements:** Elemental (C,H,N) analysis was carried out on a Perkin–Elmer PE-2400 Series **II** analyzer. – FT-IR spectra were recorded as KBr pellets on a Biorad FTS 40 spectrophotometer. – Electronic spectra for solutions were measured on a HP 8452 Diode array UV/Visible spectrophotometer. – <sup>1</sup>H-NMR measurements were conducted on a Bruker DPX 200 MHz spectrometer using TMS as the internal standard. – Cyclic voltammetric studies were conducted on BAS CV-27 and CH 660 A USA instruments. Glassy carbon was used as a working electrode, Ag/AgCl as a reference electrode, Pt wire as an auxiliary electrode and 0.1 M tetrabutylammonium hexafluorophosphate as a supporting electrolyte. – ESR investigations were carried out on a Bruker EMX spectrometer (ν = 9.75 GHz) using 100 kHz field modulation. Frequency was monitored using a microwave frequency counter in-built in the Bruker ER 041 XD-G microwave bridge. DPPH was used as a field marker (g = 2.0036). Temperature variation experiments were performed using a Bruker BVT-3000 set-up and liquid nitrogen temperature (77 K) measurements using a quartz inserting Dewar. – ESR spectral simulations were done using a Simfonia software package.

**Synthesis:** Zinc(II) tetraphenylporphyrin and its derivatives were prepared following the procedure of Adler et al.<sup>[39]</sup> Purification of the porphyrins was carried out by following the method of Barnett et al.<sup>[40]</sup> The π-cation radicals were generated by chemical oxidation of deoxygenated CH<sub>2</sub>Cl<sub>2</sub> solutions of metalloporphyrins with 0.5 equivalents of bromine in carbon tetrachloride.<sup>[33]</sup>

The complexes were characterised by various physico-chemical techniques such as elemental analysis, UV/Visible, FT-IR, FT NMR, and ESR spectroscopy, and electrochemistry. The analytical data for the various complexes are as follows:

**Zn[T(H–P)P]:** C<sub>44</sub>H<sub>28</sub>N<sub>4</sub>Zn: calcd. C 77.95, H 4.13, N 8.27; found C 77.20, H 3.99, N 8.00. – FT-IR:  $\tilde{\nu}$  = 1486 (m, C–H bend), 1339 (s, C=N stretch), 1068 (s, *p*-subst. phenyl), 1002 (vs, C–H pyrrole rock), 798 (vs, C–H out-of-plane defor.), 717 (s, mono subst. C<sub>6</sub>H<sub>5</sub>) cm<sup>−1</sup>. – UV/Vis: λ (ε), nm (cm<sup>−1</sup>·mol<sup>−1</sup>): 420 (545000), 512 (3700), 548 (25200), 586 (4600).

**Zn[T(*p*-CH<sub>3</sub>O–P)P]:** C<sub>44</sub>H<sub>36</sub>N<sub>4</sub>O<sub>4</sub>Zn: calcd. C 72.20, H 4.51, N 7.02; found C 69.54, H 5.33, N 6.75. – FT-IR:  $\tilde{\nu}$  = 1490 (m, C–H bend), 1338 (s, C=N stretch), 1246 (vs, *p*-subst. C<sub>6</sub>H<sub>5</sub>), 1106 (s, *p*-subst. phenyl), 996 (vs, C–H pyrrole rock), 801 (vs, C–H out-of-plane defor.), 718 (s, mono subst. C<sub>6</sub>H<sub>5</sub>) cm<sup>−1</sup>. – UV/Vis: λ (ε), nm (cm<sup>−1</sup>·mol<sup>−1</sup>): 422 (368000), 514 (4200), 550 (22500), 590 (8100).

**Zn[T(*m*-CH<sub>3</sub>O–P)P] · CH<sub>2</sub>Cl<sub>2</sub>:** C<sub>45</sub>H<sub>38</sub>Cl<sub>2</sub>N<sub>4</sub>O<sub>4</sub>Zn: calcd. C 66.77, H 4.34, N 6.35; found C 67.39, H 5.07, N 8.10. – UV/Vis: λ (ε), nm (cm<sup>−1</sup>·mol<sup>−1</sup>): 420 (397200), 512 (2700), 548 (18300), 584 (3100).

**Zn[T(*p*-Cl–P)P]:** C<sub>44</sub>H<sub>24</sub>N<sub>4</sub>Cl<sub>4</sub>Zn: calcd. C 64.69, H 2.96, N 6.86; found C 62.03, H 3.36, N 7.88. – FT-IR:  $\tilde{\nu}$  = 1480 (m, C–H bend), 1338 (s, C=N stretch), 1091 (s, *p*-subst. phenyl), 1000 (vs, C–H pyrrole rock), 799 (vs, C–H out of plane defor.), 723 (s, mono subst. C<sub>6</sub>H<sub>5</sub>) cm<sup>−1</sup>. – UV/Vis: λ (ε), nm (cm<sup>−1</sup>·mol<sup>−1</sup>): 420 (431300), 512 (2200), 548 (16100), 586 (2800).

**Zn[T(*m*-Cl–P)P]:** C<sub>44</sub>H<sub>24</sub>Cl<sub>4</sub>N<sub>4</sub>Zn: calcd. C 64.69, H 2.96, N 6.86; found C 63.29, H 3.13, N 7.08. – UV/Vis: λ (ε), nm (cm<sup>−1</sup>·mol<sup>−1</sup>): 420 (349800), 512 (3100), 548 (14300), 584 (2700).

**Zn[T(*p*-F–P)P]:** C<sub>44</sub>H<sub>2</sub>F<sub>4</sub>N<sub>4</sub>Zn: calcd. C 70.40, H 3.20, N 7.47; found C 69.80, H 3.85, N 8.31. – FT-IR:  $\tilde{\nu}$  = 1489 (m, C–H bend), 1337 (s, C=N stretch), 1231 (vs, *p*-subst. C<sub>6</sub>H<sub>5</sub>), 1092 (s, *p*-subst. phenyl), 1003 (vs, C–H pyrrole rock), 793 (vs, C–H out of plane defor.), 720 (s, mono subst. C<sub>6</sub>H<sub>5</sub>) cm<sup>−1</sup>. UV/Vis: λ (ε), nm (cm<sup>−1</sup>·mol<sup>−1</sup>): 420 (453400), 512 (4600), 548 (24000), 586 (4600).

## Acknowledgments

PCD thanks CSIR, New Delhi for providing Senior Research Fellowship. Financial support by The Department of Science Technology, New Delhi to DS is gratefully acknowledged.

- [1] D. Dolphin, R. H. Felton, *Acc. Chem. Res.* **1974**, 7, 26.
- [2] J. H. Dawson, *Science* **1988**, 240, 433.
- [3] C. E. Schulz, R. Rutter, J. T. Sage, P. G. Debrunner, L. P. Hager, *Biochemistry* **1984**, 23, 4743.
- [4] W. R. Browett, M. J. Stillman, *Biochim. Biophys. Acta* **1981**, 660, 1.
- [5] W. R. Patterson, T. L. Poulos, D. B. Goodin, *Biochemistry* **1995**, 34, 4342.
- [6] C. E. Schulz, P. W. Devaney, H. Winkler, P. G. Debrunner, N. Doan, R. Chiang, R. Rutter, L. P. Hager, *FEBS Letts.* **1979**, 103, 102.
- [7] R. Rutter, L. P. Hager, H. Dhonau, M. Hendrich, M. Valentine, P. Debrunner, *Biochemistry* **1984**, 23, 6809.
- [8] M. J. Benceky, J. E. Frew, N. Scowen, P. Jones, B. M. Hoffman, *Biochemistry* **1993**, 32, 11929.
- [9] J. Fajer, M. S. Davis, in: *The Porphyrins*, Part B, Vol. 4, (Ed.: D. Dolphin), Academic Press, New York, p. 197, (1979).
- [10] M. Bixon, J. Fajer, G. Feher, J. H. Freed, D. Gamliel, A. J. Hoft, H. Levanon, K. Mobius, R. Nlachushtai, J. R. Norris, A. Scherz, J. L. Sessler, D. Stehlik, *Isr. J. Chem.* **1992**, 32, 369.
- [11] W. W. Parson, B. Ke, in: *Photosynthesis: Energy Conversion by Plants and Bacteria* (Ed.: Govindjee), Academic Press, New York, **1982**, Vol. I, Ch. 8.
- [12] M. P. Gouterman in: *The Porphyrins* (Ed.: D. Dolphin), Academic Press, New York, **1978**, Vol. III, pp. 1–165.
- [13] R. S. Czernuszewicz, K. A. Macor, X.-Y. Li, J. R. Kincaid, T. G. Spiro, *J. Am. Chem. Soc.* **1989**, 111, 3860.
- [14] W. A. Oertling, A. Salehi, C. K. Chang, G. T. Babcock, *J. Phys. Chem.* **1989**, 93, 1311.
- [15] A. G. Skillman, J. R. Collins, G. H. Loew, *J. Am. Chem. Soc.* **1992**, 114, 9538.
- [16] L. K. Hanson, C. K. Chang, M. S. Davis, J. Fajer, *J. Am. Chem. Soc.* **1981**, 103, 663.
- [17] I. Fujita, L. K. Hanson, F. A. Walker, J. Fajer, *J. Am. Chem. Soc.* **1983**, 105, 3296.
- [18] M. W. Renner, R.-J. Cheng, C. K. Chang, J. Fajer, *J. Phys. Chem.* **1990**, 94, 8508.

- [19] J. E. Roberts, B. M. Hoffman, R. Rutter, L. P. Hager, *J. Biol. Chem.* **1981**, 256, 2118.
- [20] W. R. Browett, Z. Gasyne, M. J. Stillman, *J. Am. Chem. Soc.* **1989**, 110, 3633.
- [21] I. Morishima, Y. Takamuki, Y. Shiro, *J. Am. Chem. Soc.* **1984**, 106, 7666.
- [22] G. N. La Mar, V. Thanabal, R. D. Johnson, K. M. Smith, D. W. Parish, *J. Biol. Chem.* **1989**, 264, 5428.
- [23] J. R. Kincaid, Y. Zheng, J. Al-Mustafa, K. Czarnecki, *J. Biol. Chem.* **1996**, 271, 28805.
- [24] V. Palaniappan, J. Turner, *J. Biol. Chem.* **1989**, 264, 16046.
- [25] R. H. Felton, D. Dolphin, D. C. Borg, J. Jager, *J. Am. Chem. Soc.* **1969**, 91, 196.
- [26] J. Fajer, D. C. Borg, D. Forman, D. Dolphin, R. H. Felton, *J. Am. Chem. Soc.* **1970**, 92, 3451.
- [27] M. Satoh, Y. Ohba, S. Yamauchi, M. Iwaizumi, *Inorg. Chem.* **1992**, 31, 298.
- [28] Z. Gross, C. Barzilay, *Angew. Chem. Int. Ed. Engl.* **1992**, 31, 1615.
- [29] C. M. Brassily, S. A. Sibyl, T. G. Spire, Z. Gross, *Chem. Eur. J.* **1995**, 1, 222.
- [30] W. A. Kalsbeck, J. Seth, D. F. Bocian, *Inorg. Chem.* **1996**, 35, 7935.
- [31] A. G. Skillman, J. R. Collins, G. H. Loew, *J. Am. Chem. Soc.* **1991**, 114, 9538.
- [32] A. Ghosh, *J. Am. Chem. Soc.* **1995**, 117, 4691.
- [33] P. C. Dave, D. Srinivas, *J. Porphyrins and Phthalocyanines* **1998**, 2, 243.
- [34] K. Jayaraj, J. Turner, A. Gold, D. A. Roberts, R. N. Austin, D. Mandon, R. Weiss, E. Bill, M. Muther, A. X. Trautwein, *Inorg. Chem.* **1996**, 35, 1632.
- [35] A. Forman, D. C. Borg, R. H. Felton, J. Fajer, *J. Am. Chem. Soc.* **1971**, 93, 2790.
- [36] P. Bhyrappa, V. Krishnan, *Inorg. Chem.* **1991**, 30, 239.
- [37] M. J. Crossley, P. L. Burn, S. S. Chew, F. B. Cuttance, I. A. Newson, *J. Chem. Soc., Chem. Commun.* **1991**, 1564.
- [38] P. Ochsenbein, K. Ayougou, D. Mandon, J. Fischer, R. Weiss, R. N. Austin, K. Jayaraj, A. Gold, J. Turner, J. Fajer, *Angew. Chem. Int. Ed. Engl.* **1994**, 33, 348.
- [39] A. D. Adler, F. R. Longo, F. Kampas, J. Kim, *J. Inorg. Nucl. Chem.* **1979**, 32, 2443.
- [40] G. H. Barnett, M. F. Hudson, K. M. Smith, *J. Chem. Soc., Perkin Trans. I* **1975**, 1401.

Received May 3, 1999  
[199162]